A DEEP LEARNING-BASED APPROACH FOR MAPPING SHRUBS IN ARCTIC TUNDRA FROM VERY-HIGH RESOLUTION SATELLITE DATA

Darko Radakovic[1], Mark Chopping[1], Rocio Duchesne[2], Angela Erb[3], Zhuosen Wang[4] and Crystal Schaaf[3]

[1]Montclair State University, [1]radakovicd1@montclair.edu

[2]University of Wisconsin Whitewater [3]University of Massachusetts, Boston [4]University of Maryland CP/ESSIC

Objectives This study evaluated deep-learning models Convolutional Neural Network (CNN), ResNet50, VGG19, U-Net, and Vision Transformer (ViT) for detecting changes in shrub cover across Alaska's North Slope using very-high-resolution QuickBird (QB) and WorldView (WV) satellite imagery spanning 2002 to 2020. The data produced were intended to be accessible to Arctic-Boreal Vulnerability Experiment (ABoVE) researchers for evaluating the effects on summer terrestrial albedo, comparing changes in shrub abundance in Arctic tundra from the satellite very-high resolution record, verifying lower spatial resolution ABoVE remote sensing data products, and initiating, driving, calibrating and validating ecological models.

Imagery The project leveraged the availability of commercial high spatial resolution satellite imagery, including QuickBird (QB) (~ 0.6 m) from around 2005 and WorldView-2 (WV02) (~0.4 m) and WorldView-3 (WV03) (~0.3 m) from around 2013 to 2022, for diverse cloud-free, summer tundra landscapes. The Maxar Technologies (then DigitalGlobe) catalog is available to NASA Earth Science investigators, at the NASA Center for Climate Simulation (NCCS).

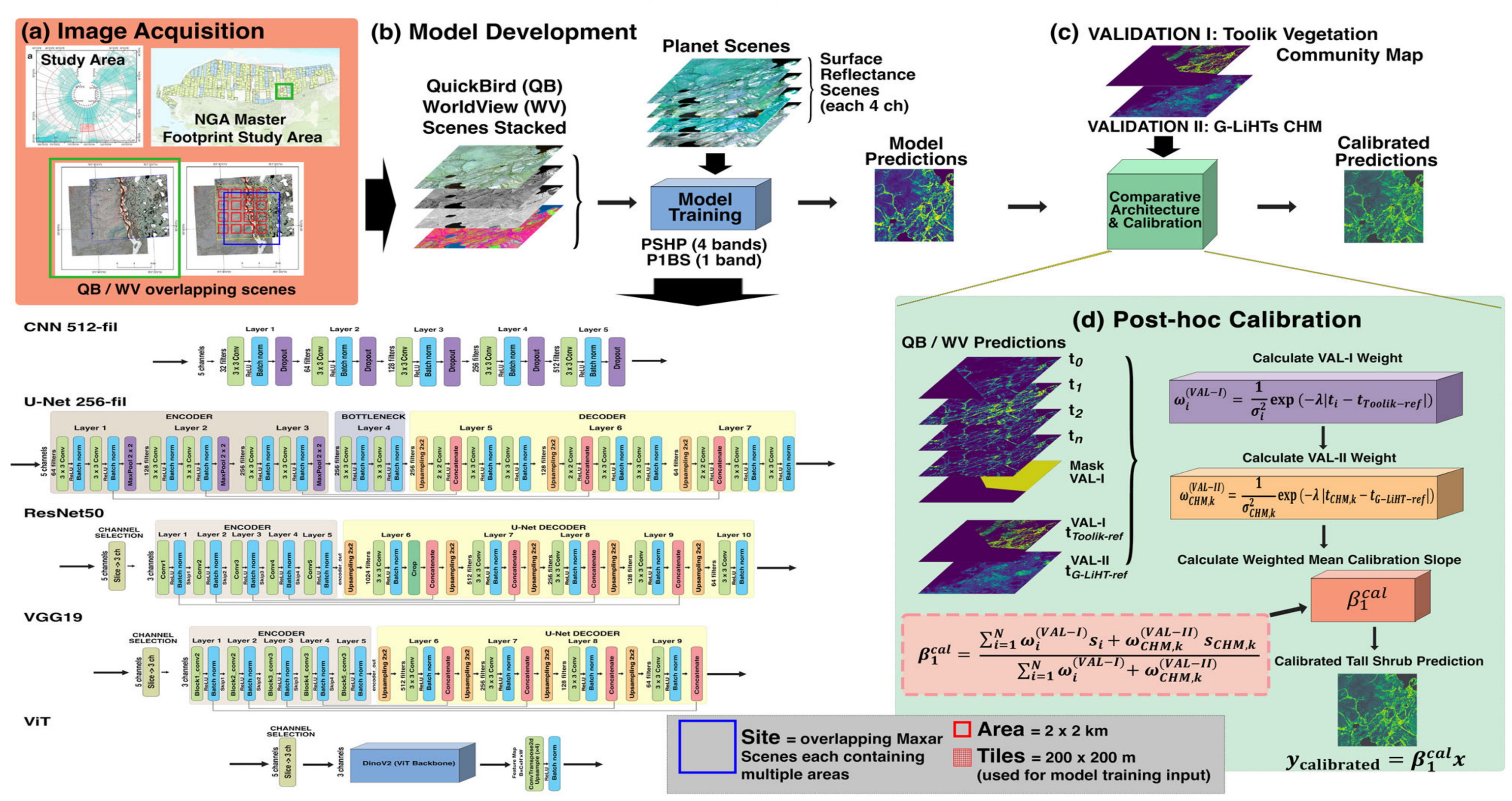

Fig 1. (a) Workflow for generating very-high-resolution deep-learning–based shrub-cover maps and an 18-year temporal change analysis. (a) image acquisition: extract overlapping 2 × 2 km QuickBird and WorldView pansharpened multispectral (PSHP; 4 channels) and panchromatic (P1BS; 1 channel) scenes (b) model development: train five architectures (CNN, U-Net, ResNet-50, VGG-19, Vision Transformer) to predict continuous shrub and wet tundra cover; and (c) validation of models and (d) post-hoc calibration of inverse-variance–weighted regression using (i) the Toolik Lake vegetation-community map [37] and (ii) Goddard's LiDAR, Hyperspectral, and Thermal (G-LiHT) canopy-height models [32] to derive a single calibration slope β_1^{cal} and produce final calibrated shrub-cover maps.

Models Models were trained on 4,100 4-band pansharpened multispectral and panchromatic image tiles (200-by-200 m) at top-of-atmosphere (TOA) radiance (Fig. 1.).

Preprocessing 2-by-2km areas from 41 study sites were subdivided in 200 x 200m x-train datasets from Pansharpened QB and WV (Fig. 1), y-train data was obtained from the Vegetation Community Map, Toolik Lake Area, Alaska, 2013-2015, which were created using high resolution Unmanned Aircraft Systems (UAS) imagery and lidar data (± 0.02m) (Greaves et al. 2018). Model performance is seen in Table 1.

TABLE 1. MODEL PERFORMANCE

Model	Acc. %	Prec. %	Rec. %	F1 %	ROC AUC %	MAE %	ME %
CNN - Shrub	85	50	60	54	80	19	3
Resnet50 - Shrub	86	52	64	57	81	18	1
U-Net - Shrub	84	45	59	51	77	22	6
VGG19 - Shrub	86	52	68	59	82	20	6
ViT - Shrub	83	46	65	54	76	20	6
CNN - Wet Tundra	69	40	57	46	70	40	17
Resnet50 - Wet Tundra	73	43	57	39	67	26	-10
U-Net - Wet Tundra	71	39	42	40	67	28	-7
VGG19 - Wet Tundra	70	36	29	31	62	28	-14
ViT - Wet Tundra	65	23	21	22	50	36	-1

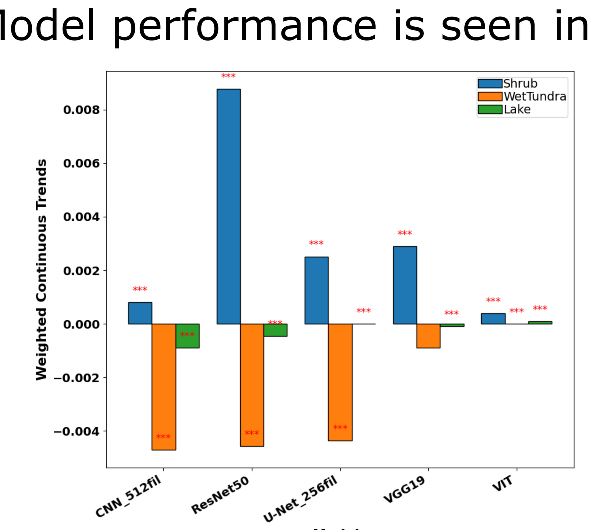

Fig. 2. Annual weighted continuous trends per model. *** p < 0.001

Calibration All imagery was orthorectified to the ABoVE Albers Conic Equal Area (Canada) grid (0.5 m) and converted to calibrated Top-of-Atmosphere (TOA) radiances using the Polar Geospatial Center's pgc_ortho.py code and Alaska DEM (alaskaned_mosaic_wgs84).

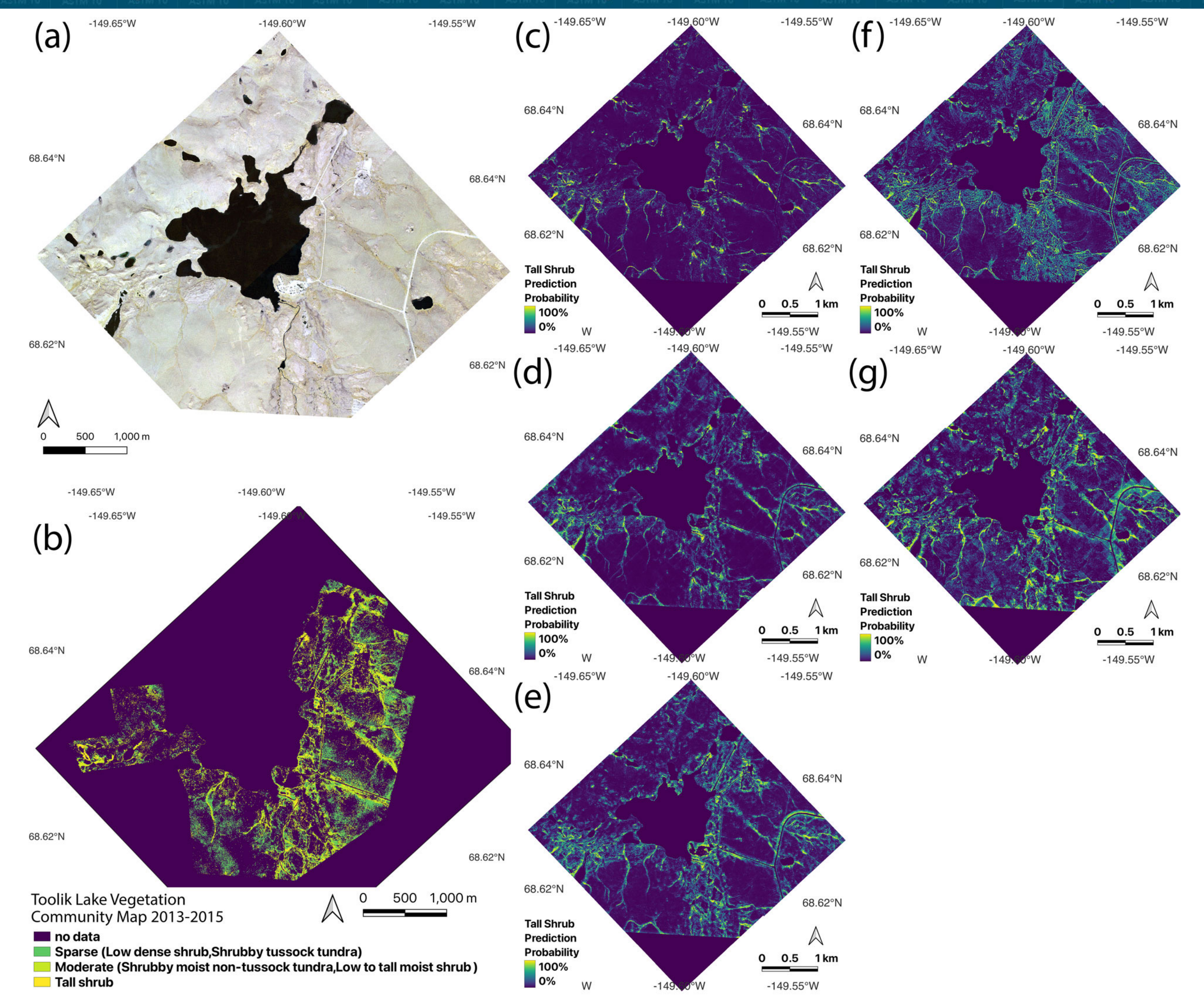

Fig. 3. (a) True-color QuickBird (QB), July 18, 2009 (QB02_20090718220421_1010010009F45F00_09JUL18220421-P1BS-500071841070_01_P001) pansharpened multispectral image of the Toolik Lake region, showing the four combined areas (1, 2, 4, 5). (b) Toolik Lake Vegetation Community validation map, which identifies major vegetation classes (classes 5, 8, 10, 11 and 12 divided into sparse, moderate and tall shrub). Panels (c) through (g) tall shrub distributions produced by (c) CNN 512-filter; (d) ResNet50; (e) VGG19; (f) U-Net 256-filter and (g) ViT. Colors indicate the model's probability of tall shrub cover, with darker shades corresponding to lower shrub presence and brighter shades corresponding to higher shrub presence. ©2009, Maxar, USG Plus

Validation All model distributions were compared against the fine scaled (~0.02 m) Toolik Lake Vegetation Community Map (Fig. 3, 4, 5), and as a second, independent validation, with the canopy height model (CHM) trained from the very-high-resolution Goddard's LiDAR, Hyperspectral, and Thermal (G-LiHT) lidar LAS data (~1 m resolution) (Fig. 7, 8) in the Yukon Flats from 2018, Alaska. Furthermore, Active Layer Thickness (ALT) from the Uninhabited Aerial Vehicle Synthetic Aperture Radar (UAVSAR) 30 m resolution from 2017 was compared with shrub cover distributions (Fig. 6 (c)) in the North Slope, Alaska.

Results ResNet50 and VGG19 achieved the highest accuracies (~86%) and balanced F1 scores for shrub segmentation. Temporal trend analyses demonstrated a significant increase in shrub cover and decrease in wet tundra and surface water bodies over time for almost all models, with the ResNet50 models showing consistently highest positive shrub trends while the CNN, VGG19, U-Net and ViT models showed more modest shrub growth (Fig. 2). Calibration against field-reference indicated strong predictive capability for ResNet50 and VGG19 models for shrub cover, with relatively low errors and biases (Fig. 7(a,b)). Comparisons with the CHM had a weak relationship (Fig. 7(c,d), Fig. 8). In addition, shrub, wet tundra cover and ALT relationships can be found in Fig. 6.

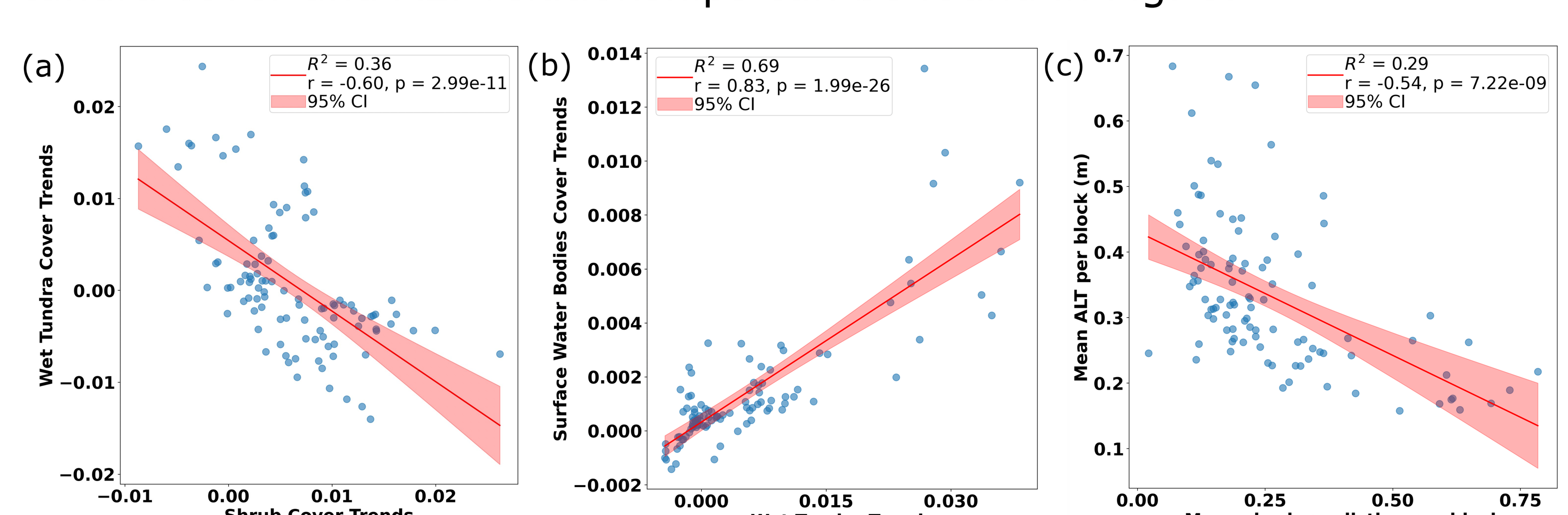

Fig. 6. (a) Negative relationship of shrub cover trends and wet tundra changes, may indicating shrub expansion coincides with decreasing wet tundra coverage, preferring moderate drainage; (b) positive relationship of wet tundra and water bodies changes, suggesting wetland drying impacts water bodies similarly; (c) negative relationship shrub cover and active layers (ALT) from 2017, likely because dense shrubs provide shading, cooler soil temperatures, or enhanced organic layer insulation, reducing soil thaw depth.

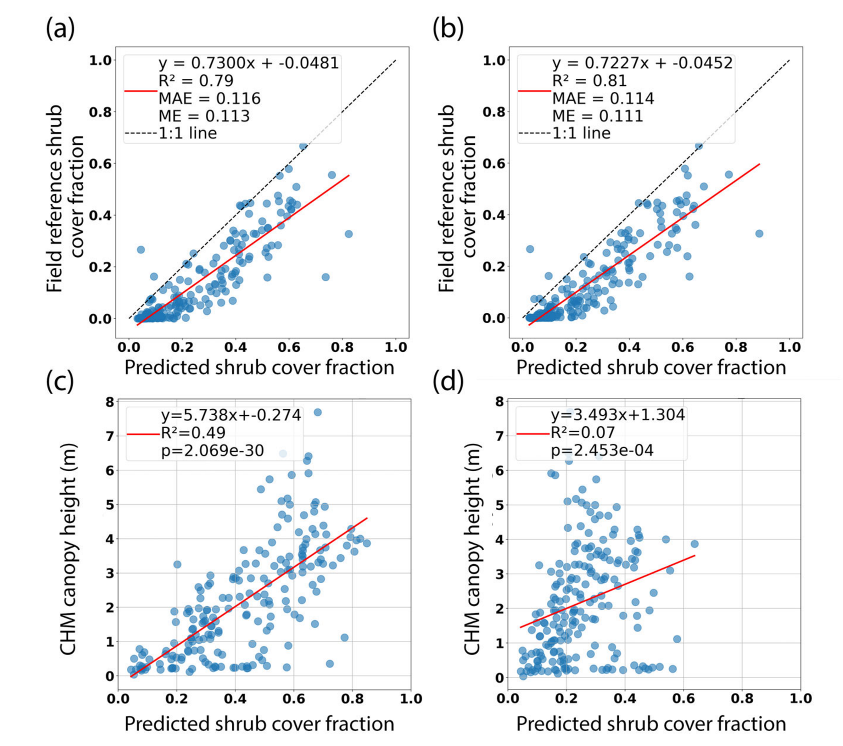

Fig. 7. Evaluation of ResNet50 and VGG19 on held-out Toolik Lake vegetation-community map data (Greaves et al., 2018). Panels (a, b): shrub cover fraction versus field reference for QuickBird-2 on QuickBird-2 on 3 July 2013; (c, d): predicted canopy height versus CHM for WorldView-3 in 2016. Shrub cover fractions aggregated into 100 × 100 m blocks; canopy height predictions into 60 × 60 m blocks. Red lines are linear regressions (R^2, MAE, ME reported in each panel); dashed grey lines indicate the one-to-one line.

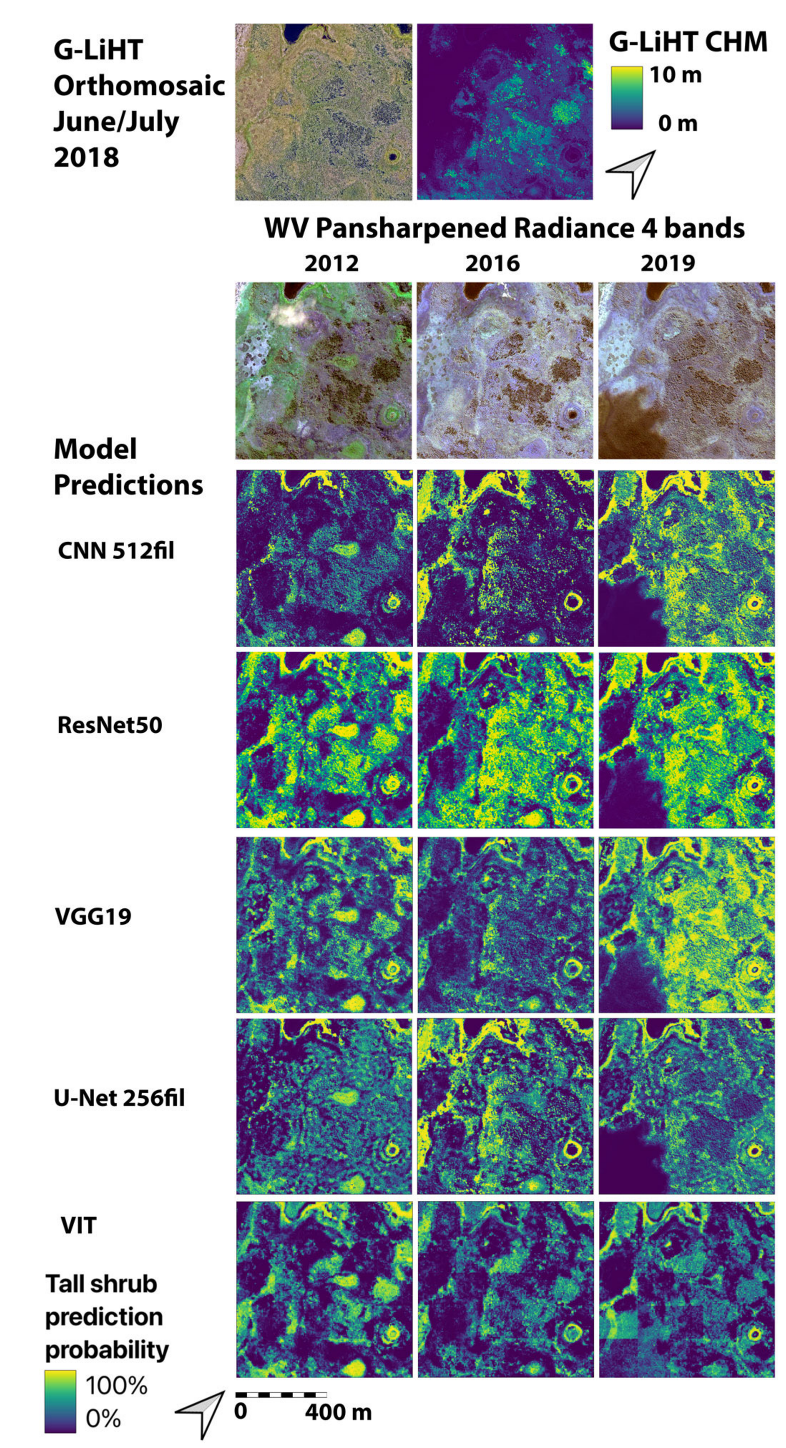

Fig. 8. Figure 60. 800 × 800 m WV predictions in the Yukon Flats, south of the North Slope, Alaska, with top row (left) showing G-LiHT orthomosaic and (right) the Canopy Height Model (CHM) up to 10 m including tall grasses, shrubs and trees (from in between 19 June – 7 July 2018). Colors in the CHM indicate the height of the vegetation, with darker shades corresponding to lower heights and brighter shades corresponding to higher heights. Second row showing RGB-color pansharpened multispectral images (left to right, WV02 2012, WV02 2016 and WV03 2019). Row three to seven show tall shrub predictions distributions produced by Maxar's CNN 512-filter, ResNet50, VGG19, U-Net 256 filters and ViT models. Colors in the predictions indicate the model's probability of tall shrub cover, with darker shades corresponding to lower shrub presence and brighter shades corresponding to higher shrub presence. Scale bars indicate 400 m. (G-LiHT: AK_20180713_Yukon_Flats_ABoVE_0_l0s4_ortho, AK_20180713_Yukon_Flats_ABoVE_0_l0s5_ortho); (WV02_20120809222239_103001001B089200_12AUG09222239-P1BS-052903604070_01_P005, WV02_20160830213545_103001005A6E6600_16AUG30213545-P1BS-501571235100_01_P001, WV03_20190801221833_1040010050B0DC00_19AUG01221833-P1BS-507215532070_01_P003) ©2012, 2016, 2019, Maxar, USG Plus

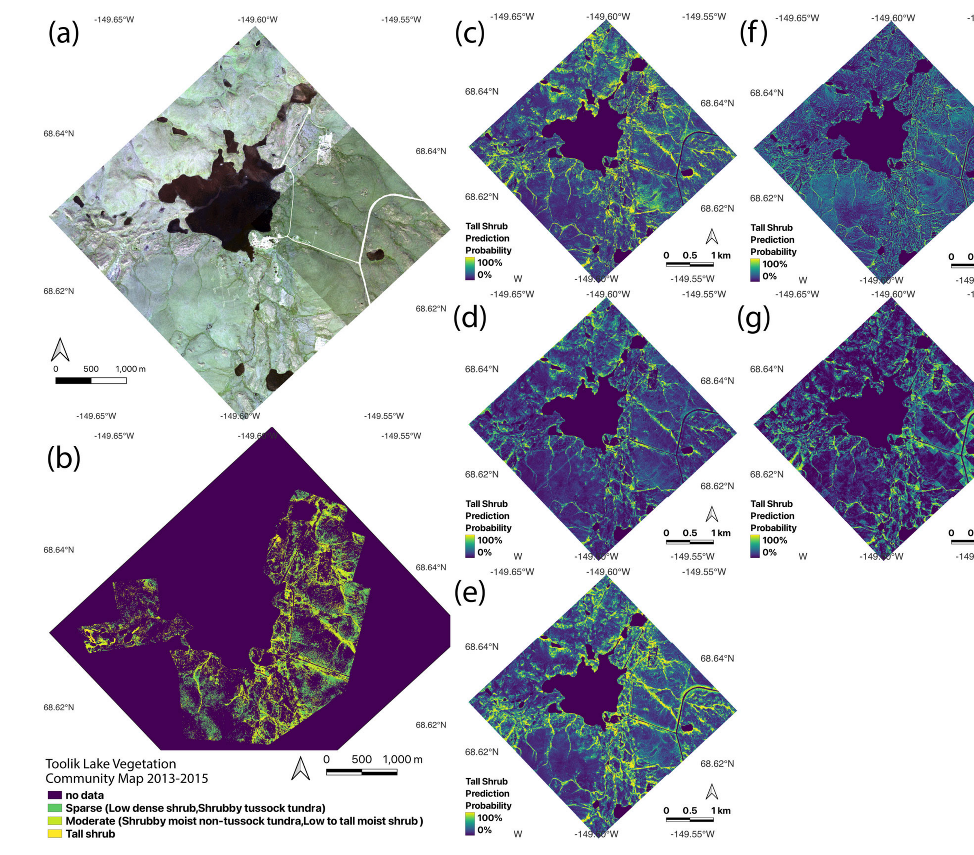

Fig. 4. (a) True-color WorldView (WV) July 14, 2016 (WV03_20160714215120_104001001F9EF500_16JUL14215120-P1BS-501553858040_01_P001) pansharpened multispectral image of the Toolik Lake region, showing the four combined areas (1, 2, 4, 5). (b) Toolik Lake Vegetation Community validation map, which identifies major vegetation classes (classes 5, 8, 10, 11 and 12 divided into sparse, moderate and tall shrub). Panels (c) through (g) tall shrub distributions produced by (c) CNN 512-filter; (d) ResNet50; (e) VGG19; (f) U-Net 256-filter and (g) ViT. Colors indicate the model's probability of tall shrub cover, with darker shades corresponding to lower shrub presence and brighter shades corresponding to higher shrub presence. ©2016, Maxar, USG Plus

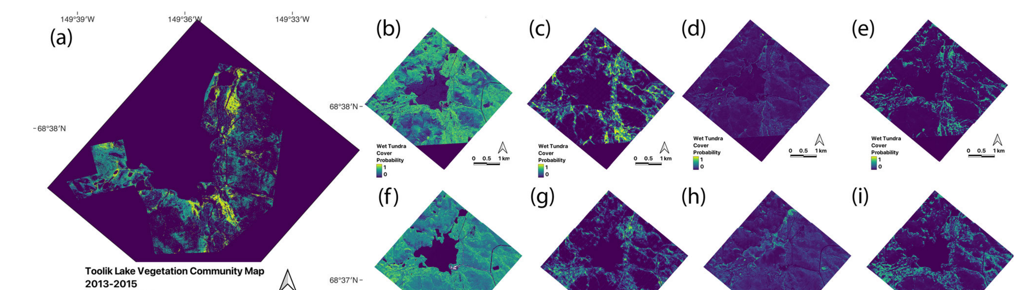

Fig. 5. (a) Toolik Lake Vegetation Community validation map, with moist and wet tundra classes (classes 6, 9, 13, 14. Panels (b)-(e) 2009 and (f)-(i) 2016 wet tundra distributions produced by CNN 512-filter; ResNet50; VGG19; U-Net 256-filter, respectively. Colors indicate the model's probability of wet tundra cover, with darker shades corresponding to lower presence and brighter shades corresponding to higher presence. (QB02_20090718220421_1010010009F45F00_09JUL18220421-P1BS-500071841070_01_P001;WV03_20160714215120_104001001F9EF500_16JUL14215120-P1BS-501553858040_01_P001 ©2009, Maxar, USG Plus)

Findings and Future Work Deep-learning segmentation of shrub cover across heterogeneous Arctic landscapes highlights that the shrub expansion aligns with documented Arctic warming trends, while preferring moderate drainage and may insulate soils by a feedback that can reduce soil thaw depth (ALT). These findings show the potential for deep-learning-based approaches to advance the understanding of permafrost dynamics and vegetation-climate feedback in rapidly changing northern ecosystems.

NASA Award 80NSSC23K1559

Acknowledgments: We gratefully acknowledge the assistance of the NASA, GSFC NCCS User Services Group (support@nccs.nasa.gov); Liz Hoy (ABoVE Science Cloud Lead, NASA, GSFC); Mark Carroll (NASA, GSFC); Clare Porter (Polar Geospatial Center); Jim Shute (NASA Center for Climate Simulation (NCCS)); Bruce Cook (NASA Goddard Space Flight Center); NASA Center for Climate Simulation (NCCS); This work utilized data made available through the NASA Commercial Satellite Data Acquisition (CSDA) Program

References

Cook, B. D., L. W. Corp, R. F. Nelson, E. M. Middleton, D. C. Morton, J. T. McCorkel, J. G. Masek, K. J. Ranson, V. Ly, and P. M. Montesano. (2013). NASA Goddard's Lidar, Hyperspectral and Thermal (G-LiHT) airborne imager. Remote Sensing 5:4045-4066, doi:10.3390/rs5084045

Greaves, H.E., L. Vierling, J. Eitel, N. Boelman, T. Magney, C. Prager, and K. Griffin. 2018. High-Resolution Shrub Biomass and Uncertainty Maps, Toolik Lake Area, Alaska, 2013. ORNL DAAC, Oak Ridge, Tennessee, USA. https://doi.org/10.3334/ORNLDAAC/1573